Original Research

Upregulation of microRNA-370 facilitates the repair of amputated fingers through targeting forkhead box protein O1

Hongxing Zhang[1,*], Xiaojuan Sun[2,*] and Dingjun Hao[3]

[1]Department of Hand Surgery, Xi'an Honghui Hospital, Xi'an Jiaotong University Health Science Center, Xi'an 710054, China;
[2]Department of Anesthesiology, Xi'an Honghui Hospital, Xi'an Jiaotong University Health Science Center, Xi'an 710054, China;
[3]Department of Spine Surgery, Xi'an Honghui Hospital, Xi'an Jiaotong University Health Science Center, Xi'an 710054, China
*The first two authors contributed equally to this study
Corresponding author: Dingjun Hao. Email: dingjunhao029@163.com

Abstract

Angiogenesis is critical to the success of digital replantation. Recent study suggests an important regulatory role of microRNA-370 (miR-370) in ischemia–reperfusion injury. However, its function in digital replantation is poorly understood. In this study, we reported that the expression of miR-370 was upregulated in replantation tissues. miR-370 mimic transfection promoted human umbilical vein endothelial cells (HUVECs) proliferation by regulating the cell cycle and inhibited apoptosis. miR-370 mimic transfection also significantly increased HUVECs migration and induced the formation of capillary-like structures in HUVECs, indicated that miR-370 promoted capillary tube formation *in vitro*. Furthermore, forkhead box protein O1 (FOXO1) was identified as the functional target of miR-370 by dual-luciferase reporter assay. FOXO1 overexpression vector lacked 3′-UTR together with miR-370 mimic transfection strongly abrogated miR-370-induced cell proliferation and the formation of capillary-like structures in HUVECs. Taken together, our results revealed that the upregulation of miR-370 might facilitate the repair of amputated fingers by regulating angiogenesis through targeting FOXO1. This study provided a potential therapeutic target for the restoration of finger function after replantation.

Keywords: Digital replantation, microRNA-370, proliferation, forkhead box protein O1, angiogenesis

***Experimental Biology and Medicine* 2016; 241: 282–289. DOI: 10.1177/1535370215600549**

Introduction

In 1965, Komatsu and Tamai reported the first successful digital replantation.[1,2] In the past 50 years, the advent of microsurgery has led to the replantation of almost every amputated part such as the distal phalanx (fingertip). Despite advances in microsurgical techniques and instruments, avulsion and crush injuries in the replantation of digits and hand in many cases are still contraindicated. The goals of replantation are to restore circulation and regain sufficient function and sensation of the amputated part, as well as to allow patients to return to their previous employment.[3]

The presence of a functional vasculature is essential to the viability of nearly all tissues. The importance of the capillary bed to tissue survivability is highlighted when tissue injury repair occurs. In healing wounds, an initial vigorous angiogenic response results in a vessel density that far exceeds that of normal tissue.[4] Optimum healing of a cutaneous wound requires a well-orchestrated integration of the complex biological and molecular events involved in cell migration, proliferation, angiogenesis, and remodeling.[5,6] Among many factors, angiogenesis or re-vascularization is an important natural process during wound healing. It has previously been shown that the vascular supply differs in regenerating and non-regenerating amputated rodent digits,[7] and revascularization in the amputated digit is thought to be crucial for improved digit regeneration.

MicroRNAs (miRNAs) are a class of endogenous, 20–25 bp non-coding RNAs that regulate gene expression by acting on target mRNAs for translational repression or degradation.[8,9] It has been reported that miRNAs act as critical regulators in many different aspects of homeostasis, development, and disease.[10,11] Recently, several miRNAs have been described in vascular development and vascular disorders/diseases. miRNAs have been found to play important roles in angiogenesis and vascular disease via regulating vascular cell migration, proliferation, and apoptosis through their target genes.[12,13] miR-370 is a recently discovered miRNA that plays important regulatory roles in the morphogenesis of diverse organs[14] and several

human tumors.[15–18] Recent results have shown that miR-370 is upregulated in hepatic ischemia reperfusion injury, and inhibition of miR-370 efficiently attenuates hepatic ischemia reperfusion injury. Further studies have revealed that miR-370 plays a potential role in hepatic ischemia–reperfusion injury by targeting transforming growth factor-β receptor II.[19] However, the role of miR-370 in digital replantation has seldom been reported.

In this study, we examined the expression of miR-370 during recovery after digital replantation. We also explored the effect of miR-370 on the development and progression of angiogenesis. The potential targets of miR-370 during this process were also studied by further analysis.

Materials and methods

Human tissue

Primary human amputate tissues and replantation tissues were obtained from patients who underwent surgery at Xi'an Honghui Hospital. The tissue biopsies were taken from the damaged tissues which should be cut during debridement. This study was approved by the institutional review board and was conducted in accordance with an assurance filed with and approved by Xi'an Honghui Hospital. Written informed consent was obtained from all patients/patient family members enrolled in the present study. The replantation success was evaluated according to the standard of clinical curative efficacy evaluation of orthopedic.[20] Tissues were preserved by snap-freezing and stored at −80°C for subsequent protein and RNA extraction with TRIZOL reagent for qRT-PCR analysis as per the manufacturer's instructions.

Cell culture

Human umbilical vein endothelial cells (HUVECs) were obtained from Lonza (Allendale, NJ) and maintained in M-199 medium (Gibco/Invitrogen, Carlsbad, CA) supplemented with 20% fetal bovine serum (FBS; Gemini Bio-Products, West Sacramento, CA), 1% penicillin/streptomycin (Gibco/Invitrogen), 50 μg/mL endothelial cell growth supplement (ECGS; BD Biosciences, San Jose, CA), and cultured at 37°C in 5% CO_2.

Plasmids and dual-luciferase reporter assay

The forkhead box protein O1 (FOXO1) expression vectors (wild-type and phosphorylation deficient mutants) and FOXO1-luciferase constructs have been described elsewhere. Briefly, the fragment from the 3′-UTR of FOXO1 mRNA containing the predicted miR-370 binding sequences was cloned into the SacI/XmaI sites of the pGL3 luciferase promoter vector (Promega, Madison, WI). The primers were: FOXO1-3′-UTR-wt-up: 5′-GC CCCGCGGCTTCAGATTGTCTGACAGCAGGAAC-3′; FO XO1-3′-UTR-wt-dn: 5′-GCCCTGCAGATGGCACAGTC CTTATCTACAGC-3′; FOXO1-3′-UTR-mu-up: 5′-GCCC CGCGGCTTCAGATTGTCTGACAGCACCAAC-3′ and FOXO1-3′-UTR-mu-dn: 5′-GCC CTGCAGATGGCACA GTCCTTATCTACAGC-3′.

HUVECs were seeded at 1×10^5 cells per well in a 96-well plate and transfected with 200 ng of the different plasmid DNAs using GenePORTER 2™ (Gene Therapy Systems, San Diego, CA) according to the manufacturer's instructions. Lysates were harvested 36 h after transfection, and the reporter activity was measured with the Dual Luciferase Assay (Promega). The relative luciferase activities were normalized to that of the control cells.

MiR-370 mimic transfection

The miR-370 mimic and negative control were purchased from RiboBio (Guangzhou, Guangdong, China). For studies in 96-well plates, miR-370 mimic were resuspended in 50 μL of Lipofectamine 2000/Opti-MEM (Invitrogen Life Technologies) and added to the relevant plates before the addition of HUVECs (1×10^5) and incubation at 37°C for 4 h. The transfection effect of miR-370 mimic was determined by quantitative real-time PCR (qRT-PCR).

Construction of FOXO1 overexpression vector

FOXO1 cDNA sequence without the 3′-UTR, which can escape miR-370 regulation, was amplified from cDNA derived from HUVECs. The PCR product was digested with *EcoRI* and *BglII* and cloned into *BamH1/EcoR1*-digested FUGW vector. Primers used were 5′-GGC GGATCCATGGCCGAGGCGCCTC-3′ and 5′-GGCGAA TTCTCAGCCT-GACACCCAGCTATGT-3′.
LipofectamineTM 2000/Opti-MEM (Invitrogen Life Technologies) was used for the transfection.

qRT-PCR

TRIzol reagent (Invitrogen) was used to extract total RNA according to the manufacturer's instructions. RNA was eluted in 50 μL of RNase-free water (Promega) and stored at −70°C. miRNA expression profiling was conducted on total RNA extracts by the two-step TaqMan RT-PCR protocol. To analyze gene expression, the qRT-PCR mixture system containing cDNA templates, primers, and SYBR Green qPCR Master Mix were subjected to qRT-PCR according to standard methods. The primers for p21Cip1 (forward: 5′-CGATGCCAACCTCCTCAACGA-3′ and reverse: 5′-TCGCAGACCTCCAGCATCCA-3′), cyclin D1 (forward: 5′-AACTACCTGGACCGCTTCCT-3′ and reverse: 5′-CC ACTTGAGCTTGTTCACCA-3′), and β-actin (forward: 5′-GACTCATGACCACAGTCCATGC-3′ and reverse: 3′-AGAGGCAGGGATGATGTTCTG-5′) were used. Data were normalized to the levels of β-actin. For miR-370 analysis, a TaqMan microRNA assay kit (Applied Biosystems, Foster City, CA) was used. U6 ribosomal RNA was used as the internal control. The cDNA was obtained by reverse transcription PCR using a miR-370-specific primer, and the primers for miR-370 amplification were 5′-GG CGAATTCTGCATTCCTCATTCTAC-3′ and reverse, 5′-GC GCTCGAGTAACGTCTCTGTGCCTG-3′. The changes in results were calculated with the formula $R = 2^{\Delta\Delta CT}$.

Cell proliferation

Cell viability was assessed by using the 3-(4,5-dimethylthiazol-2-yl)-2,5-diphenyltetrazolium bromide (MTT) assay. Cells (2×10^3 cells/well) were cultured in 96-well plates and given fresh media every other day. Cells were then transfected with miR-370 mimic or the negative control as described above for 24 h. During the last 4 h of each day of culture, cells were treated with MTT (50 mg per well, Sigma, St. Louis, MO). Dimethyl sulfoxide was used to dissolve the formazan and the absorbance was measured at 450 nm using an ELISA plate reader (Bio-tek, Winooski, VT).

HUVECs migration assay

The migration ability of HUVECs was tested in a Transwell Boyden Chamber (6.5 mm, Costar). The polycarbonate membranes (8 mm pore size) on the bottom of the upper compartment of the Transwells were coated with 0.1% gelatin matrix. Cells were suspended in serum-free vascular cell basal medium at a concentration of 4×10^5 cells/mL, then added to the upper chamber (4×10^5 cells/well). Simultaneously, 0.5 mL of medium with 10% FBS was added to the lower compartment, and the Transwell-containing plates were incubated for 4 h in a 5% CO_2 atmosphere saturated with H_2O. At the end of the incubation, cells that had migrated to the lower surface of the filter membrane were fixed with 90% ethanol for 15 min at room temperature, washed three times with distilled water, and stained with 0.1% crystal violet in 0.1 mol/L borate and 2% ethanol for 15 min at room temperature. Cells remaining on the upper surface of the filter membrane (non-migrant) were scraped off gently with a cotton swab. Cell migration was quantified by blind counting of the migrated cells on the lower surface of the membrane, with five fields per chamber.

Flow cytometric analysis of apoptosis

To investigate cell apoptosis, we performed flow cytometric analysis of phosphatidylserine externalization using the Annexin V-fluorescein isothiocyanate kit (Immunotech, Marseille, France). HUVECs were starved of serum and growth factors by culturing in M199 with 5% 0.22-μm filtered MP-free FCS for 16 h. Following treatment, cells were harvested and washed once with ice-cold phosphate-buffered saline, and then re-suspended in binding buffer (10 mmol/L HEPES, pH 7.4, 150 mmol/L NaCl, 2.5 mmol/L $CaCl_2$, 1 mmol/L $MgCl_2$, 4% bovine serum albumin). Annexin V-fluorescein isothiocyanate (0.5 μg/mL) and propidium iodide (PI; 0.6 μg/mL) were added to a 250 μL aliquot (5×10^6 cells) of this cell suspension. After incubation in the dark at room temperature for 15 min, stained cells were immediately analyzed on a FACS Calibur™ (Becton Dickinson).

Matrigel assay

Angiogenesis assays were performed *in vitro*. Matrigel was purchased from Chemicon, and the assays were performed according to the manufacturer's manual. Briefly, HUVECs with different treatment were cultured for 48 h, serum starved overnight, then trypsinized, and subjected to the Matrigel assay. Quantification of branch points per field (20×) was done on six fields and six sample repeats.

Western blotting

Cells or limb tissues were lysed with loading lysis buffer that was diluted from 5× loading lysis buffer (0.5 mol/L Tris–HCl [pH 6.8] 2.5 mL, dithiothreitol 0.39 g, sodium dodecyl sulfate (SDS) 0.5 g, bromophenol blue 0.025 g, glycerin 2.5 mL). Equal amount of protein was transferred onto the polyvinylidene fluoride (PVDF) membrane. The membrane was then incubated with primary antibodies against p21 (Cell Signaling Technology, Danvers, MA), cyclin D1 (Cell Signaling Technology), FOXO1 (Abcam, Cambridge, MA), and β-actin (Cell Signaling Technology) 4°C for 1 h. Then the membranes were incubated with horseradish peroxidase (HRP)-conjugated secondary antibodies (Sigma) for 1 h at room temperature. The binding signals were visualized by enhanced chemiluminescence (ECL; Thermo Fisher Scientific, UK).

Statistical analysis

All experiments were repeated at least three times. The results are expressed as mean ± SD values. The differences between groups were determined using two-tailed Student's *t*-tests and one-way ANOVAs in the software SPSS version 12.0 (SPSS). A *P*-value <0.05 was considered to be statistically significant.

Results

MiR-370 was highly expressed during the replantation of amputated fingers

The expression of miR-370 was analyzed in amputated and replantation tissues from six patients. The patients' finger replantation healing outcome at two months following surgery was shown in Figure 1a. During this process, qRT-PCR analysis revealed that miR-370 expression was markedly increased in replantation tissues, compared to amputated tissue ($P < 0.05$, $n = 6$, Figure 1b). Together, this result indicated that miR-370 might play a role in the healing of replantation of amputated fingers. We also determined the expression levels of FOX01, one of potential targets of miR-370. It was demonstrated that the protein expression level of FOX01 was decreased in all the replantation tissues ($P < 0.05$, $n = 6$, Figure 1c).

The effect of miR-370 on the proliferation, apoptosis, migration, and angiogenesis of HUVECs

In order to investigate the role of miR-370 in the replantation of fingers, we transfected miR-370 mimic into HUVECs. A significant increase of miR-370 expression was observed after miR-370 mimic transfection as determined by qRT-PCR (Figure 2a). The MTT assay demonstrated that the proliferation of miR-370 mimic transfected cells was dramatically increased compared to the control group (Figure 2b). Additionally, Western blotting analysis demonstrated that the expression levels of the CDK

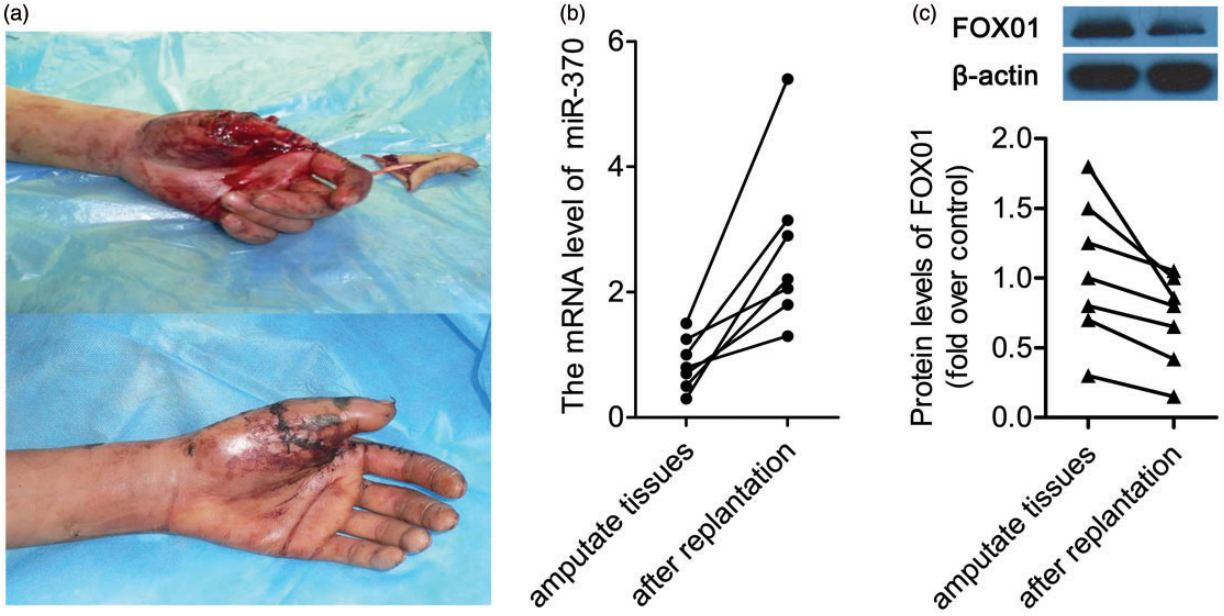

Figure 1 The level of miR-370 is higher after the replantation of amputated tissues. (a) A representative picture of a hand immediately following surgery and outcome after surgery. Up: hand immediately after injury; Down: the outcome after surgery at two months. (b) qRT-PCR analysis of miR-370 expression in amputated tissues and tissues after replantation. Data are presented as mean ± SD, $n = 6$. $P < 0.05$ *vs*. amputated tissues. (c) The protein expression levels of FOX01 in amputated tissues and replantation tissues were determined by Western blot. Up: a representative blot of FOX01 protein expression. Down: the quantitative data of FOX01 protein expression determined by Western blot. Data were presented as mean ± SD, $n = 6$. $P < 0.05$ *vs.* amputated tissues. (A color version of this figure is available in the online journal.)

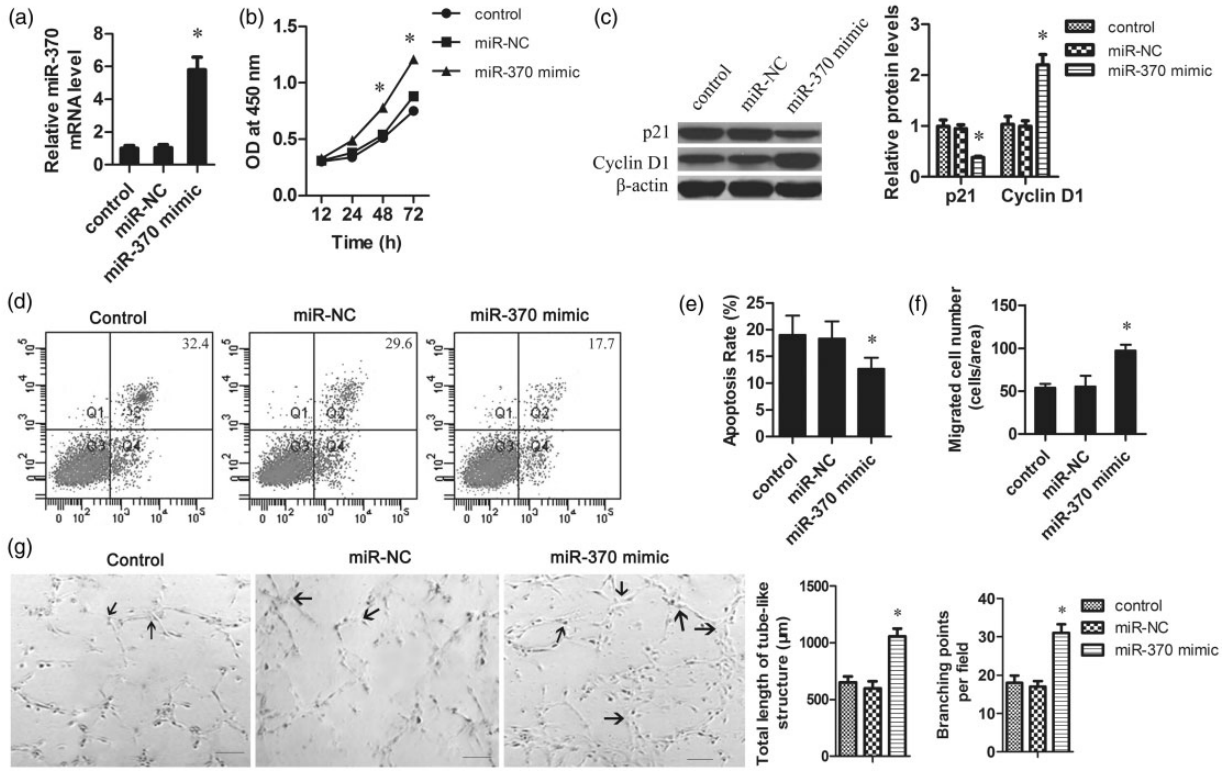

Figure 2 The effect of miR-370 on the proliferation, apoptosis, migration, and angiogenesis of HUVECs. HUVECs were seeded at 1×10^5 cells per well in a 96-well plate. The miR-370 mimic or negative control was transfected into the HUVECs using Lipofectamine 2000. (a) Four hours post transfection, the mRNA levels of miR-370 in HUVECs were determined by qRT-PCR. The data were normalized according to β-actin. (b) MTT assays revealed that the overexpression of miR-370 promoted the growth of HUVECs. (c) Total protein was isolated from HUVECs with different treatments. The protein levels of p21 and cyclin D1 were measured by Western blot. β-Actin was used as the loading control. (d) Representative pictures of cells apoptosis determined by flow cytometry. Apoptosis of serum-starved HUVECs was analyzed by annexin V-fluorescein isothiocyanate and PI staining. (e) Quantification of apoptotic cells. (f) The migration ability of HUVECs was tested in a Transwell Boyden Chamber. (g) Representative pictures of Matrigel assays after overexpression of miR-370 in HUVECs. Endothelial network formation on Matrigel was quantified at 48 h from cell seeding. Angiogenesis was evaluated using Matrigel assays *in vitro*. The total length of tube-like structures and the number of branching points were quantified. Arrows indicated the capillary branch points. Scale bar 50 μm. *$P < 0.05$ *vs*. control group

inhibitor p21Cip1 were downregulated and cyclin D1 protein was upregulated in miR-370-transfected cells, compared to the control group (Figure 2c). These results indicated that upregulation of miR-370 might promote the proliferation of HUVECs by regulating the expression of cell cycle-related proteins.

To determine the function of miR-370 on cell apoptosis, HUVECs were transfected with miR-370 mimic and serum starved for 24 h. As shown in Figure 2d, overexpression of miR-370 reduced the apoptosis rate triggered by serum starvation. Quantification analysis confirmed that the cell apoptosis rate was significantly decreased by miR-370 mimic transfection (Figure 2e). These results suggest that miR-370 might be involved in the repair process during digital replantation by attenuating endothelial cell (EC) apoptosis.

The migration capacity of HUVECs was assessed to explore the effect of miR-370 on angiogenesis. Overexpression of miR-370 strongly enhanced HUVEC migration across Transwell filters (Figure 2f). To verify the effect of miR-370 on angiogenesis, the planar Matrigel assay was used to investigate the function of miR-370 in EC network formation. When cultured on Matrigel, overexpression of miR-370 induced the formation of capillary branch points and tube-like structures in HUVECs (Figure 2g), indicated that miR-370 promoted angiogenesis formation *in vitro*.

miR-370 targeted FOXO1 in HUVECs

Potential targets of miR-370 were searched by both TargetScan and PicTar. As shown in Figure 3a, there was a potential binding site of miR-370 located on the 3′-UTR of FOXO1. It was showed that miR-370 mimic transfection did not affect the mRNA level of FOXO1 (Figure 3b), but significantly decreased the protein level of FOXO1 (Figure 3c). To confirm the function of the putative miR-370 binding site in the FOXO1-3′-UTR, we subcloned the 3′-UTRs of FOXO1 into the pGL3 dual-luciferase reporter vectors and luciferase activity was measured. Transfection of miR-370 reduced the luciferase activity of the FOXO1-3′-UTR luciferase reporter plasmid in HUVECs (Figure 3d). Furthermore, the repressive effect of miR-370 on the FOXO1-3′-UTR was abrogated by point mutations in the miR-370-binding seed region of the FOXO1-3′-UTR. These results demonstrated that FOXO1 was a bona fide target of miR-370.

Overexpression of FOXO1 abrogated miR-370-induced angiogenesis

To further understand the role of FOXO1 in miR-370-induced angiogenesis in the repair process of digital replantation, a FOXO1 overexpression vector without the 3′-UTR, which could escape miR-370 regulation, was constructed, and was then transfected into miR-370-overexpressing HUVECs. FOXO1 was significantly increased both in mRNA and protein level as compared to control group or miR-370 mimic sole transfection group (Figure 4a and b). The co-transfection with FOXO1 restored the inhibitory effect of miR-370 on the expression of p21Cip1 (Figure 4c and d). At the same time, the high expression of cyclin D1 induced by miR-370 upregulation was obviously decreased

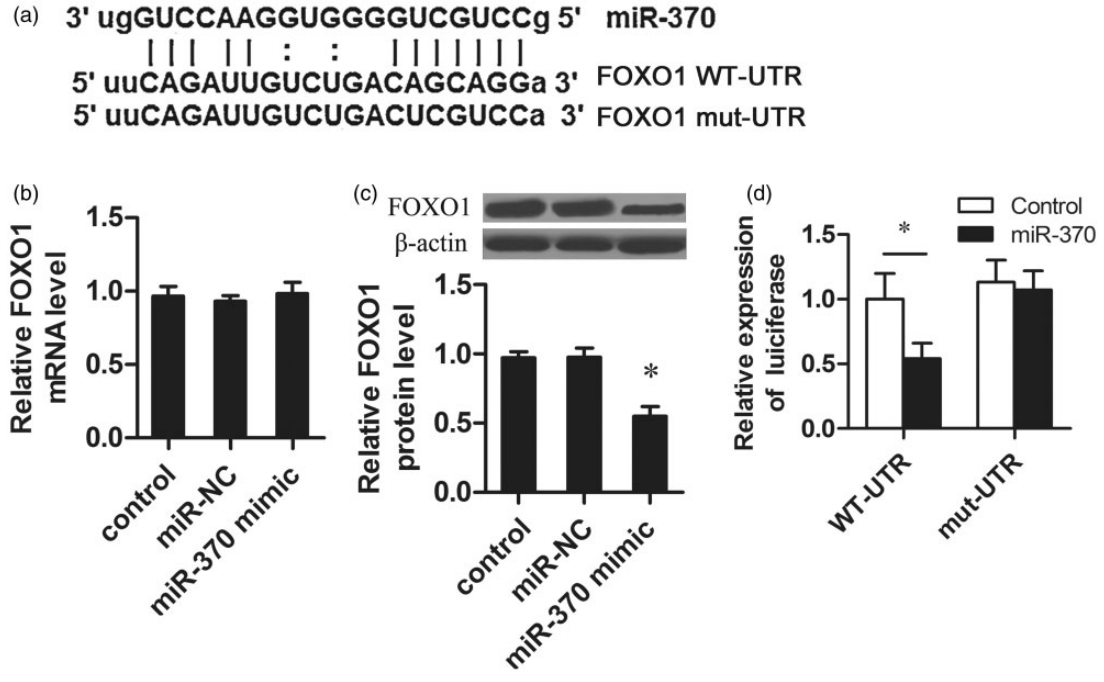

Figure 3 MiR-370 downregulated FOXO1 expression by directly targeting the FOXO1 3′-UTR. (a) Predicted miR-370 target sequences in the 3′-UTR of FOXO1. Mutant FOXO1 means the 3′-UTR containing mutated nucleotides. (b) HUVECs seeded at 1 × 105 cells per well in a 96-well plate were transfected with miR-370 mimic or negative control using Lipofectamine 2000. The mRNA level of FOXO1 was detected by qRT-PCR. (c) Total protein was isolated from HUVECs transfected with miR-370 mimic or negative control. The protein expression of FOXO1 was detected by Western blot. (d) The fragment from the wild type or the mutant 3′-UTR of FOXO1 mRNA containing the predicted miR-370 binding sequences was cloned into the pGL3 luciferase promoter vector. The miR-370 mimic was co-transfected into the cells with 3′-UTR sequence. Reporter activity was measured with the Dual Luciferase Assay. *$P < 0.05$

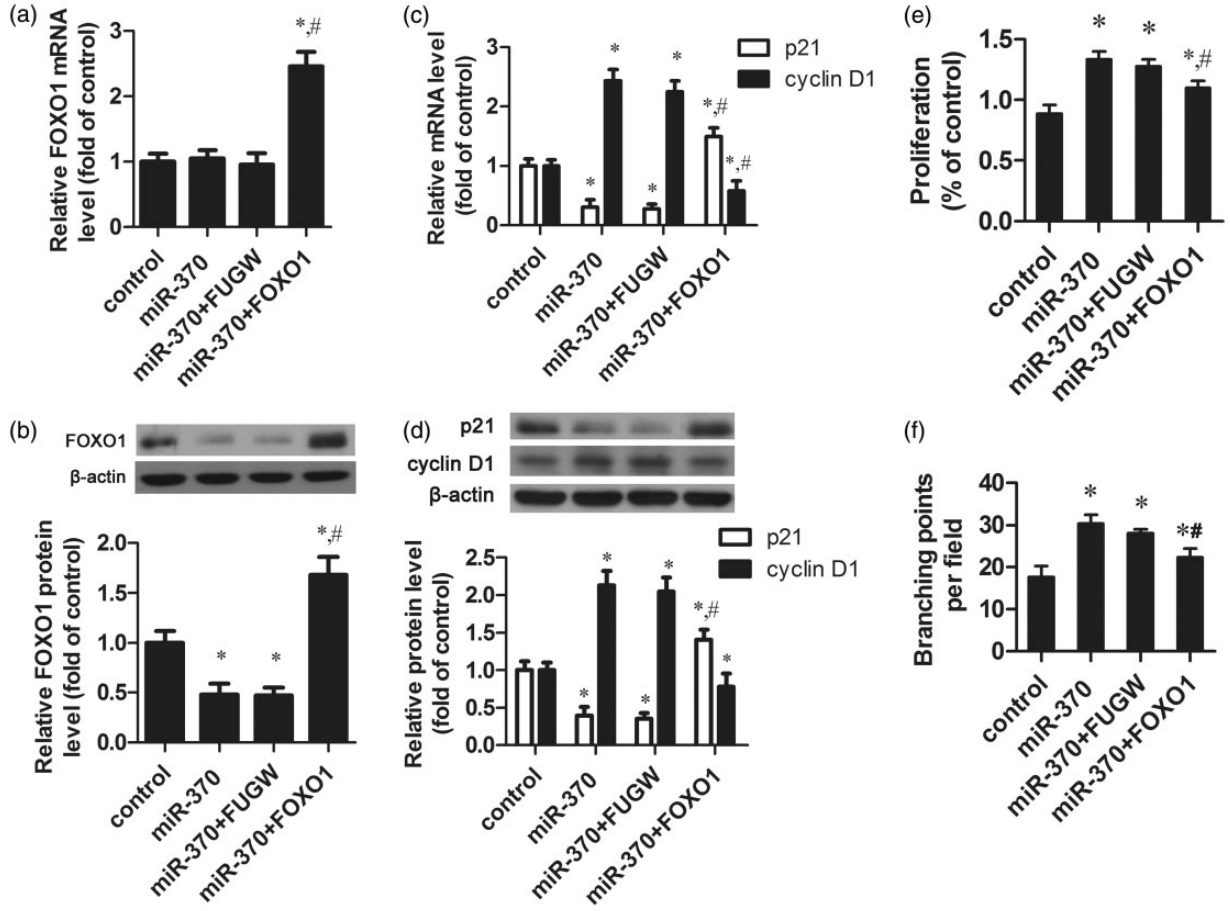

Figure 4 FOXO1 plays an important role in miR-370-induced HUVECs proliferation, resistance to apoptosis and angiogenesis. HUVECs were transfected with sole miR-370 mimic (miR-370), both miR-370 mimic and empty vector (miR-370 + FUGW), both miR-370 mimic and FOXO1 overexpression vector lacked 3′-UTR (miR-370 + FOXO1). (a) The mRNA levels of FOXO1 were measured by qRT-PCR. β-actin was used as the internal control. (b) The protein levels of FOXO1 were measured by Western blot. β-Actin was used as the internal control. (c, d) The mRNA and protein levels of p21Cip1 and cyclin D1 were determined by qRT-PCR and Western blot, respectively. (e) Cell proliferation was measured by MTT assay. (f) Quantification of the formation of branching points *in vitro*. $^{*}P < 0.05$ *vs*. control group. $^{\#}P < 0.05$ *vs*. miR-370 group

after FOXO1 overexpression (Figure 4c and d). The MTT assay also showed that co-transfection with FOXO1 significantly slowed the growth rate of HUVECs compared to miR-370 overexpressing cells (Figure 4e). The Matrigel assay showed that FOXO1 inhibited the capillary morphogenesis in HUVECs induced by the overexpression of miR-370 (Figure 4f). Collectively, the evidence suggests that miR-370 might play a role in angiogenesis in the repair process of digital replantation by targeting FOXO1.

Discussion

There is increasing evidence that miRNAs are involved in various biological processes, such as skeletal muscle proliferation and differentiation, oncogenesis, brain morphogenesis, and hematopoietic lineage differentiation.[21–24] miR-370 has been reported to play a regulatory role in several tumors, such as acute myeloid leukemia, gastric cancer, and cholangiocarcinoma.[20–23] It is known that many of these miRNAs are associated with wound healing, including the angiogenesis of repair, such as pro-angiogenic miR-130, miR-27b, miR-220, the miR-17-92 cluster and anti-angiogenic miR-221 and miR-222.[25–27] Among these, miR-370 has been revealed to have important functions in hepatic ischemia-reperfusion injury, suggesting that it may play a role in the repair process. In this study, we demonstrate that miR-370 is upregulated in replantation tissues, compared to amputated tissue, indicating that miR-370 may exert a potential role in promoting regeneration during the healing of replantation tissues. However, in which cell type did miR-370 express was still not clear.

There is a growing emphasis on restoration of finger function after replantation, while circulatory function is also an important aspect. The formation of new blood vasculature from preexisting vessels, a process called angiogenesis, is essential to wound healing. Recent studies have shown that angiogenesis is a critical and complex event in the wound-healing process, such as brain and bone repair.[28] EC activation, proliferation, migration, and maturation have been shown to play an important role in the growth of blood vessels and subsequent injury repair. HUVECs are a valuable model of angiogenesis *in vitro* because of their ability to form capillary-like structures called tubes in response to appropriate stimuli. To further

investigate the role of miR-370 in digital replantation, we explored the impact of miR-370 on angiogenesis. As expected, miR-370 increased HUVECs proliferation and decreased apoptosis. Importantly, miR-370 overexpression induced cell migration and the formation of capillary-like structures. Collectively, these findings suggest that miR-370 may facilitate digital replantation by promoting angiogenesis.

FOXO1 family is an established regulator of cell-cycle inhibition, metabolism, and apoptosis.[29–32] FOXO1 is a critical regulator of embryonic vascular development and could maintain vascular homeostasis.[33] Recent studies have demonstrated that FOXO1 is regulated by miR-370 in prostate cancer cells and gastric carcinoma cells.[17] To further investigate the role of miR-370 in digital replantation, we analyzed the effect of FOXO1 on miR-370-mediated angiogenesis. In this study, overexpression of miR-370 decreased FOXO1 protein expression. Here, we also demonstrated that FOXO1 is a target gene of miR-370 in HUVECs. Further analysis confirmed that overexpression of FOXO1 abrogated miR-370-induced cell proliferation by regulating the cell–cycle inhibitor p21Cip1 and the cell-cycle regulator cyclin D1. Importantly, FOXO1 upregulation reduced the formation of capillary-like structures induced by miR-370. All these results show that miR-370 can promote angiogenesis by directly targeting FOXO1.

In conclusion, the key finding of the current study is that miR-370 is highly expressed in replantation tissues. Importantly, this research suggests that miR-370 may regulate the repair process of digital replantation by enhancing angiogenesis by directly targeting FOXO1. Accordingly, miR-370 may act as a potential novel therapeutic target for the restoration of finger function after replantation.

Author contributions: HZ and DH conceived and designed the experiments. HZ and DH performed the experiments. DH, HZ, and XS analyzed the data. HZ and XS contributed reagents/materials/analysis tools. HZ, XS, and DH wrote the paper.

ACKNOWLEDGMENTS

The author(s) received no financial support for the research, authorship, and/or publication of this article.

DECLARATION OF CONFLICTING INTEREST

The author(s) declared no potential conflicts of interest with respect to the research, authorship, and/or publication of this article.

REFERENCES

1. Masuhara K, Tamai S, Fukunishi H, Obama K, Komatsu S. [Experience with reanastomosis of the amputated thumb]. *Seikeigeka Orthop Surg* 1967;**18**:403–4
2. Komatsu S, Tamai S. Successful replantation of a completely cut-off thumb. *Plast Reconstr Surg* 1968;**42**:374–7
3. Beris AE, Lykissas MG, Korompilias AV, Mitsionis GI, Vekris MD, Kostas-Agnantis IP. Digit and hand replantation. *Arch Orthop Trauma Surg* 2010;**130**:1141–7
4. DiPietro LA. Angiogenesis and scar formation in healing wounds. *Curr Opin Rheumatol* 2013;**25**:87–91
5. Martin P. Wound healing–aiming for perfect skin regeneration. *Science* 1997;**276**:75–81
6. Falanga V. Wound healing and its impairment in the diabetic foot. *The Lancet* 2005;**366**:1736–43
7. Said S, Parke W, Neufeld DA. Vascular supplies differ in regenerating and nonregenerating amputated rodent digits. *Anat Rec Part A* 2004;**278**:443–9
8. Bartel DP. MicroRNAs: genomics, biogenesis, mechanism, and function. *Cell* 2004;**116**:281–97
9. Kim VN, Nam J-W. Genomics of microRNA. *Trends Genet* 2006;**22**:165–73
10. Ambros V. The functions of animal microRNAs. *Nature* 2004;**431**:350–55
11. Erson A, Petty E. MicroRNAs in development and disease. *Clin Genet* 2008;**74**:296–306
12. Urbich C, Kuehbacher A, Dimmeler S. Role of microRNAs in vascular diseases, inflammation, and angiogenesis. *Cardiovasc Res* 2008;**79**:581–8
13. Zhang C. MicroRNAs in vascular biology and vascular disease. *J Cardiovasc Translat Res* 2010;**3**:235–40
14. Qi L, Hongjuan H, Ning G, Zhengbin H, Yanjiang X, Tiebo Z, Zhijun H, Qiong W. miR-370 is stage-specifically expressed during mouse embryonic development and regulates Dnmt3a. *FEBS Lett* 2013;**587**:775–81
15. Zhang X, Zeng J, Zhou M, Li B, Zhang Y, Huang T, Wang L, Jia J, Chen C. The tumor suppressive role of miRNA-370 by targeting FoxM1 in acute myeloid leukemia. *Mol Cancer* 2012;**11**:56
16. Lo S, Hung P, Chen J, Tu H, Fang W, Chen C, Chen W, Gong N, Wu C. Overexpression of miR-370 and downregulation of its novel target TGFβ-RII contribute to the progression of gastric carcinoma. *Oncogene* 2011;**31**:226–37
17. Wu Z, Sun H, Zeng W, He J, Mao X. Upregulation of MircoRNA-370 induces proliferation in human prostate cancer cells by downregulating the transcription factor FOXO1. *PloS One* 2012;**7**:e45825
18. Meng F, Wehbe-Janek H, Henson R, Smith H, Patel T. Epigenetic regulation of microRNA-370 by interleukin-6 in malignant human cholangiocytes. *Oncogene* 2007;**27**:378–86
19. Li L, Li G, Yu C, Shen Z, Xu C, Feng Z, Zhang X, Li Y. A role of microRNA-370 in hepatic ischaemia-reperfusion injury by targeting transforming growth factor-β receptor II. *Liver Int*, Epub ahead of print 2014)
20. Xieyuan J. *The standard of clinical curative efficacy evaluation of orthopaedic*. Beijing: People's Medical Publishing House, 2005
21. Zhao Y, Samal E, Srivastava D. Serum response factor regulates a muscle-specific microRNA that targets Hand2 during cardiogenesis. *Nature* 2005;**436**:214–20
22. Chen J-F, Mandel EM, Thomson JM, Wu Q, Callis TE, Hammond SM, Conlon FL, Wang D-Z. The role of microRNA-1 and microRNA-133 in skeletal muscle proliferation and differentiation. *Nat Genet* 2005;**38**:228–33
23. Chen C-Z, Li L, Lodish HF, Bartel DP. MicroRNAs modulate hematopoietic lineage differentiation. *Science* 2004;**303**:83–6
24. Esquela-Kerscher A, Slack FJ. Oncomirs—microRNAs with a role in cancer. *Nat Rev Cancer* 2006;**6**:259–69
25. Suárez Y, Fernández-Hernando C, Pober JS, Sessa WC. Dicer dependent microRNAs regulate gene expression and functions in human endothelial cells. *Circ Res* 2007;**100**:1164–73
26. Kuehbacher A, Urbich C, Zeiher AM, Dimmeler S. Role of Dicer and Drosha for endothelial microRNA expression and angiogenesis. *Circ Res* 2007;**101**:59–68
27. Poliseno L, Tuccoli A, Mariani L, Evangelista M, Citti L, Woods K, Mercatanti A, Hammond S, Rainaldi G. MicroRNAs modulate the angiogenic properties of HUVECs. *Blood* 2006;**108**:3068–71
28. Li J, Zhang YP, Kirsner RS. Angiogenesis in wound repair: angiogenic growth factors and the extracellular matrix. *Microsc ResTech* 2003;**60**:107–14
29. Hanafusa H, Torii S, Yasunaga T, Nishida E. Sprouty1 and Sprouty2 provide a control mechanism for the Ras/MAPK signalling pathway. *Nat Cell Biol* 2002;**4**:850–58

30. Salih DA, Brunet A. FoxO transcription factors in the maintenance of cellular homeostasis during aging. *Curr Opin Cell Biol* 2008;**20**:126–36
31. Fu Z, Tindall D. FOXOs, cancer and regulation of apoptosis. *Oncogene* 2008;**27**:2312–9
32. Sengupta A, Molkentin JD, Paik J-H, DePinho RA, Yutzey KE. FoxO transcription factors promote cardiomyocyte survival upon induction of oxidative stress. *J Biol Chem* 2011;**286**:7468–78
33. Paik J-H, Kollipara R, Chu G, Ji H, Xiao Y, Ding Z, Miao L, Tothova Z, Horner JW, Carrasco DR. FoxOs are lineage-restricted redundant tumor suppressors and regulate endothelial cell homeostasis. *Cell* 2007;**128**:309–23

(Received April 27, 2015, Accepted July 21, 2015)